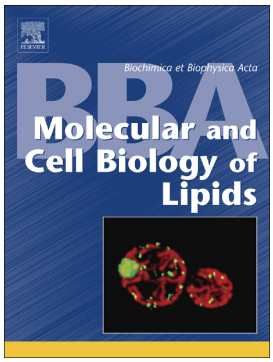

X-box binding protein 1 (XBP1): A key protein for renal osmotic adaptation. Its role in lipogenic program regulation

Cecilia Casali, Ricardo Malvicini, Luciana Erjavec, Leandro Parra, Ayelen Artuch, María C. Fernández Tome

PII: S1388-1981(20)30008-1

DOI: https://doi.org/10.1016/j.bbalip.2020.158616

Reference: BBAMCB 158616

To appear in: *BBA - Molecular and Cell Biology of Lipids*

Received date: 10 September 2019

Revised date: 26 December 2019

Accepted date: 7 January 2020

Please cite this article as: C. Casali, R. Malvicini, L. Erjavec, et al., X-box binding protein 1 (XBP1): A key protein for renal osmotic adaptation. Its role in lipogenic program regulation, *BBA - Molecular and Cell Biology of Lipids*(2020), https://doi.org/10.1016/j.bbalip.2020.158616

X-box binding protein 1 (XBP1): a key protein for renal osmotic adaptation. Its role in lipogenic program regulation.

Cecilia Casali[*,1,2], Ricardo Malvicini[*1], Luciana Erjavec[1,2], Leandro Parra[1,2], Ayelen Artuch[1] and María C. Fernández Tome [1,2**].

* These authors contributed equally to this work.

1. Universidad de Buenos Aires, Facultad de Farmacia y Bioquímica, Departamento de Ciencias Biológicas, Cátedra de Biología Celular y Molecular. Buenos Aires. Argentina

2. Universidad de Buenos Aires. Consejo Nacional de Investigaciones Científicas y Técnicas. Instituto de Química y Fisicoquímica Biológicas Prof. Dr. Alejandro C. Paladini (IQUIFIB)-Facultad de Farmacia y Bioquímica, Buenos Aires. Argentina

Cecilia Irene Casali, e-mail address: ccasali@ffyb.uba.ar

Ricardo Malvicini, e-mail address: ricardomalvi@gmail.com

Leandro Gastón Parra, e-mail address: le.parra@live.com

Luciana Cecilia Erjavec, e-mail address: luerjavec@gmail.com

Ayelen Artuch, e-mail address: ayelenartuch@gmail.com

María C. Fernández Tome, e-mail address: fertome@ffyb.uba.ar

**Corresponding Author:
Dr. Fernández Tome, María C.
Departamento de Ciencias Biológicas,
Biología Celular y Molecular,
Facultad de Farmacia y Bioquímica, UBA
IQUIFIB, CONICET
Junín 956, 1er piso, (C1113AAD)
Ciudad Autónoma de Buenos Aires, ARGENTINA.
Phone number: +5411-5287-4784
email: fertome@ffyb.uba.ar

Author Contributions:

CC and RM performed the experiments; LE designed primers and analysed data; LP analyzed data; AA contributed with PCR experiments, CC and MCFT conceived and supervised the study; CC and MCFT wrote the manuscript. All authors discussed the results and commented on the manuscript

Abstract

In renal cells, hyperosmolarity can induce cellular stress or differentiation. Both processes require active endoplasmic reticulum (ER)-associated protein synthesis. Lipid biosynthesis also occurs at ER surface. We showed that hyperosmolarity upregulates glycerophospholipid (GP) and triacylglycerol (GL-TG) de novo synthesis. Considering that massive synthesis of proteins and/or lipids may drive to ER stress, herein we evaluated whether hyperosmolar environment induces ER stress and the participation of inositol-requiring enzyme 1α (IRE1α)-XBP1 in hyperosmotic-induced lipid synthesis. Treatment of Madin-Darby canine kidney (MDCK) cells with hyperosmolar medium triggered ER stress-associated unfolded protein response (UPR). Hyperosmolarity significantly increased *xbp1* mRNA and protein as function of time; 24 h of treatment raised the spliced form of XBP1 protein (XBP1s) and induced its translocation to nuclear compartment where it can act as a transcription factor. XBP1 silencing or IRE1α ribonuclease (RNAse) inhibition impeded the expression of lipin1, lipin2 and diacylglycerol acyl transferase-1 (DGAT1) enzymes which yielded decreased GL-TG synthesis. The lack of XBP1s also decreased sterol regulatory element binding protein (SREBP) 1 and 2. Together our data demonstrate that hyperosmolarity induces IRE1α→XBP1s activation; XBP1s drives the expression of SREBP1 and SREBP2 which in turn regulates the expression of the lipogenic enzymes lipin1 (LPIN1) and 2 (LPIN2) and DGAT1. We also demonstrated for the first time that tonicity-responsive enhancer binding protein (TonEBP), the master regulator of osmoprotective response, regulates XBP1 expression. Thus, XBP1 acts as an osmoprotective protein since it is activated by high osmolarity and upregulates lipid metabolism, membranes generation and the restoration of ER homeostasis

Key words:
Hyperosmolarity, ER stress, lipogenic enzymes, XBP1, SREBP.

Abbreviations:
UPR, unfolded protein response; XBP1, X-box binding protein; GP, glycerophospholipids; GL-DG, diacylglycerol; GL-TG, triacylglycerol; LD, lipid droplets; SREBP, sterol regulatory element binding protein; TonEBP, tonicity-responsive enhancer binding protein; DGAT, diacylglycerol acyltransferase;

1. Introduction.

Hyperosmolarity is a key controversial signal for renal cells. Under physiological conditions, it induces renal cell differentiation and maturation of urine concentrating system. High interstitial osmolarity is necessary to concentrate urine in mature kidneys [1-3]. However, abrupt changes in environmental osmolarity may induce cell stress that can lead to death. Interestingly, both processes require an active synthesis of proteins either related to renal function in differentiated cells or related to osmoprotection [2-5]. In addition, we demonstrated that hyperosmolarity upregulates lipid metabolism in renal cells, by activating the transcription of lipogenic genes such as fatty acid synthase (*fas*), lipins, diacylglycerol acyltransferase (*dgat*) and the transcriptional regulator sterol regulatory element-binding protein (*srebp*) [6-8]. Hyperosmolar activation of lipid metabolism is a requirement as an osmoprotective mechanism by preserving membrane structure as well as a physiological tool in differentiation by constructing cell structure and tissue architecture.

Most lipids, glycerophospholipids (GP), trilglycerols (GL-TG), cholesterol and ceramide biosynthesis occur at the endoplasmic reticulum (ER). In addition, ER plays a central role in calcium storage and homeostasis, and in membrane-, secretory- and lysosomal-proteins synthesis, folding and post-translational modifications [9, 10]. In response to several stimuli, an abrupt protein synthesis may occur leading to an accumulation of macromolecular aggregates of misfolded proteins within ER lumen, which causes the disruption of ER homeostasis, known as ER stress. To restore ER homeostasis, the unfolded protein response (UPR) is activated. The UPR is an intracellular signaling pathway that transmits signals from the ER lumen in order to activate gene transcription. As consequence of UPR activation, ER protein-folding capacity is improved by increasing the expression of chaperones and foldases as well as the expansion of the ER membranes. If ER stress is not resolved, cell death occurs [11]. ER stress activates UPR by means of three ER transmembrane transducers: the inositol-requiring enzyme kinase 1α (IRE1α), the pancreatic ER kinase (PERK), and the activating transcription factor 6 (ATF6). In normal conditions, all these three proteins bind to a chaperone named binding immunoglobulin protein (BiP), also known glucose-regulated protein 78 (GRP78), through their luminal domains. Under stress conditions, BiP binds to misfolded proteins causing its dissociation from IRE1α, ATF6 and/or PERK. These proteins suffer a conformational change that triggers UPR pathways signaling. All the three pathways promote the transcription of genes related to

the restoration of cell homeostasis [11].

Activated-IRE1α pathway drives IRE1α-endoribonuclease (RNase) activation which initiates a non-conventional mRNA splicing reaction of the pre-existing X box binding protein 1 mRNA *(xbp1u).* Spliced-XBP1 mRNA *(xbp1s)* is then translated to the spliced XBP1 protein (XBP1s). XBP1s is a transcription factor that translocates to the nucleus and initiates the transcription of UPR-related and non-related genes. XBP1expression is also activated by ATF6 and PERK pathways [11]. XBP1s can be considered a super transcription factor since its activity is associated with the expression of chaperones, endoplasmic reticulum-associated degradation (ERAD) proteins, XBP1 itself and inflammatory genes [12]. XBP1s also mediates the expression of genes involved in differentiation, survival, apoptosis and autophagy. In addition, IRE1α-XBP1s pathway is involved in lipid metabolism since activates the transcription of many lipogenic enzymes such as DGAT2 (diacylglycerol acyl transferase 2), SCD1 (stearoyl-CoA desaturase 1) and ACC2 (Acetyl-CoA carboxylase 2), being a critical regulator of hepatic lipid metabolism [13] .

Bearing in mind this background information, the aim of the present work was to determine whether hyperosmolarity activates IRE1α/XBP1s pathway in renal epithelial cells and the role of XBP1s transcription factor in the upregulation of lipid metabolism in renal cells submitted to hyperosmolar stress.

2. Materials and Methods

All drugs, salts and solvents used to prepare buffers or chromatography mobile phases were of analytical grade and purchased from Merck Argentina.

2.1. Culture conditions. Madin-Darby canine kidney (MDCK) cells (American Type Culture Collection, passages 55–58) were grown in a mixture containing DMEM (Dulbecco's modified eagle's medium) and Ham's-F12 (1:1) (GIBCO^{TM}), 10 % FBS (Fetal bovine serum) (Natocor^{TM}), and 1 % antibiotic mixture (GIBCO^{TM}). After reaching 70–80% confluence, cells were placed in low-serum medium (0.5% FBS) for 24 h and then subjected to hyperosmolarity for different periods of time (0, 6, 12, 24 or 48 h). For isosmolar condition, the commercial medium was used. Its osmolality (298 ± 19 mOsmol/Kg of water), measured with an osmometer (μOSMETTE, Precision Systems; Sudsbury, MA), resulted from its sodium salts composition: 120 mM NaCl, 14 mM $NaHCO_3$, 0.5 mM Na_2HPO_4 (anhydrous), 0.5 mM $NaH_2PO_4 \cdot H_2O$. Hyperosmolar media were made by adding aliquots of sterile 5 M NaCl to commercial medium to achieve desired final osmolality (520 ± 12 mOsmol/Kg of water) generated by sodium salts of commercial medium plus the addition of 125 mM NaCl [6, 14]. After treatments, media containing dead cells and debris were discarded, and cells attached to the culture plastic were collected after 0.25 % trypsin-EDTA (GIBCO^{TM}) treatment and counted in a hemocytometer chamber (Neubauer´s chamber). Total and viable cells were determined by trypan blue exclusion test which is based on the principle that live cells possess intact cell membranes that exclude trypan blue whereas not viable cells do not [15]. Cells were used for western blot analysis, mRNA isolation and cellular fractionation.

2.2. Analysis of XBP1 contribution to lipid synthesis. The involvement of XBP1 in glycerophospholipids (GP) and triglycerol-glycerolipids (GL-TG) synthesis was evaluated by using 4μ8C (Sigma-Aldrich), a pharmacological inhibitor of IRE1α-associated endoribonuclease activity which is involved in the splicing of the immature *xbp1* mRNA (*xbp1u)* [16]; or by gene silencing using *xbp1*-small interfering RNA (*xbp1*-siRNA) strategy. To do this, MDCK cells were grown in a mixture containing DMEM/Ham's-F12 (1:1), 10 % FBS and 1 % antibiotic mixture. After reaching 70–80% confluence, cells were placed in low-serum medium (0.5% FBS) for 24 h and, before NaCl addition, cultures were grown in the absence or in the presence of 20 μM 4μ8C for 30 min to allow

inhibitor uptake. After that, hyperosmolar cultures were made by supplementing media with 5 M NaCl up to final concentration 125 mM while isosmolar cultures were added with equal volume of sterile vehicle. Then cells were incubated for extra 24 h.

In other set of experiments, cells were transfected with *xbp1*-siRNA designed in our laboratory by using BLOCK-iT™ RNAi Designer (Thermofisher) (5'CCUCUGAGACAGAGAGCCAAGCUAA-3'/5'-UUAGCUUGGCUCUCUGUCUCAGAGG-3') and purchased from Invitrogen. Transfections were performed with lipofectamine 3000 (Invitrogen) according to manufacturer instructions. Briefly, MDCK cells were grown in a mixture containing DMEM/Ham's-F12 (1:1), 10 % FBS and 1 % antibiotic mixture. After reaching 50% confluence, media were replaced by fresh DMEM-F12/0.5 % FBS without antibiotic containing a mixture of lipofectamine 3000 and an aliquot of 20 μM *xbp1*-siRNA to reach final concentration of 40 nM. Cells were grown in the presence of this reactive for 5 h and then, transfection protocol was repeated once. After transfection, media were replaced by fresh DMEM-F12/0.5 % FBS and hyperosmolar cultures were made by supplementing media with 5 M NaCl up to final concentration 125 mM, while isosmolar cultures were added with equal volume of sterile vehicle. Then cells were incubated for extra 24 h. After treatments, cells were collected by 0.25 % trypsin-EDTA treatment, counted and used for RNA extraction or for lipid metabolism analysis.

2.3. Analysis of TonEBP participation in lipogenic genes expression. To evaluate the role of TonEBP transcription factor on lipogenic enzyme expression, *tonebp* gene was silenced before hyperosmolar treatment by using *tonebp*-siRNA duplex (5′AUGGGCGGUGCUUGCAGCUCCUU3′/ 5′GGAGCUGCAAGC ACCGCCCAUU 3', Invitrogen) designed by Na et al [17]. MDCK cells were grown in a mixture containing DMEM/Ham's-F12 (1:1), 10 % FBS and 1 % antibiotic mixture. After reaching 50% confluence, media were replaced by fresh DMEM-F12/0.5 % FBS without antibiotic containing a mixture of lipofectamine 3000 and an aliquot of 20 μM *tonebp*-siRNA to reach final concentration of 200 nM. Cells were grown in the presence of this mixture for 5 h and then, transfection protocol was repeated once. After transfection, media were replaced by fresh DMEM-F12/0.5 % FBS and hyperosmolar cultures were made by supplementing media with 5 M NaCl up to final concentration 125 mM, while isosmolar cultures were added with equal volume of sterile vehicle. Then cells were incubated for extra 24 h. After treatments, cells were collected by 0.25 % trypsin-EDTA treatment, counted and used for RNA extraction.

2.4. RNA isolation and RT-PCR analysis. MDCK cells were grown in a mixture containing DMEM/Ham's-F12 (1:1), 10 % FBS and 1 % antibiotic mixture. After reaching 70-80 % confluence, cells were subjected to hyperosmolar media for different periods of time (6, 12, 24, 48 h, as it is described in 2.1.); or treated with IRE1α-associated endoribonuclease activity inhibitor 4μ8C (as described in 2.2); or transfected with *xbp1*-siRNA or *tonebp*-siRNA (as described in 2.2 and 2.3.) and then treated with hyperosmolar medium and incubated for extra 24 h. Once the incubation time had finalized, cells were trypsinized, collected and counted as described above (see 2.1.). In all treatments, 2×10^6 cells were used for total RNA extraction by means of the SV Total RNA Isolation System (Promega) in accordance with the manufacturer's instructions. First-strand cDNA was synthesized from total RNA by using MMLV retrotranscriptase (Promega) and oligodT (Biodynamics). To evaluate mRNA expression level, cDNA PCR amplification was done by using specific primers designed with Primer3 software (BioTools - University of Massachusetts Medical School). *β-actin* was used as loading control. Table 1 shows primers sequences, the number of cycles applied and the annealing temperature in each case. PCR products were resolved in 2 % agarose (Promega) gels containing ethidium bromide (Promega) prepared in TBE (90 mM Tris/Borate/3 mM EDTA) buffer. The presence of PCR products was revealed under UV light. Bands densitometries were performed with Gel Analyzer 19.1 online-free software.

Table 1. Nucleotide sequences for specific primers used in PCR assays.

Protein	Primer Forward (5´→3´)	Primer Reverse (5´→3´)	Cycles	TA (ºC)
BGT1	GAGGTAGTCCCTAGTCCCACA	CACCCACAAAGTCCAGAGGT	28	58
COX2	TCAGCCATACAGCAAATCCTT	GTAGCACTAGTAGTTTAGGAGT	25	55
SMIT	GCTCATAGCCAAAGGCTCTAC	TCACCACCATAAAAGCCACA	25	58
β-Actin	CAAAGCCAACCGTAGAGAAG	CAGAGTCCATAGACAATACCAG	24	58
XBP1	ACTAGCCAGAGACCGAAAGAA	TCTCCGCCTCCTCTTCAGTA	24	58
XBP1(s)	ACCCTAGGCTACTAGAAGAGGA	TCAACGCTAGTCAGAATCCAT	31	59.1
CHOP	CCCTCACTCTCCAGATTCCA	TAGCCACTTTCCTCTCGTTCT	26	58
BIP	TCACCTCCTAGGGAACTTTTAG	TTTAGTCTTCAGCGGTCACAC	26	58
Lipin1	CGCAAGTCCTTCAGGTTCTC	TGTGGAGATGACTTTGCAGC	28	64.5
Lipin2	AAGACCAAAATAGCTTCCCCT	TAGATCCCCAGAATAGGAAGAG	29	63.6
DGAT1	TGGATAGTGAGCCGCTTCTT	AGGAGCCTCATAGTGGAGCA	32	60.8
DGAT2	AGTAGGCTCAGGCAGGTTAGA	GATAGCTCTTCAAAATAGGGGA	32	63.6
SREBP1	AGACATGGCAACCACTGTGA	GARAGRRCCRCCGCTCACCA	31	59.1
SREBP2	GATGTCATCTGTCGGTGGTG	GGGGGCTCRCTGRRACTTCC	28	59.1
TonEBP	AAGGCAACTCAAAAGCAGGA	CCTGCAACACTACTGGCTCA	26	58

2.5. Metabolic labeling experiments. In order to evaluate the role of XBP1s in glycerolipid synthesis we studied the incorporation of [U-^{14}C]-glycerol (Perkin-Elmer ™) into GP, GL-TG and GL-DG in MDCK cells treated either with 4μ8C or *xbp1*-siRNA. To do that, MDCK cells were grown in a mixture containing DMEM/Ham's-F12 (1:1), 10 % FBS and 1 % antibiotic mixture. After reaching 70–80% confluence, cells were placed in low-serum medium (0.5% FBS) for 24 h and, before NaCl addition, cultures were grown in the absence or in the presence of 20 μM 4μ8C for 30 min to allow inhibitor uptake. After that, MDCK cells without or with 4μ8C were incubated in commercial media (isosmolar condition controls) or in hyperosmolar media for extra 24 h. In other set of experiments, cells were transfected with *xbp1*-siRNA as described in 2.2. and after transfection treatment, media were replaced by fresh DMEM-F12/0.5 % FBS alone (isosmolar condition) or added with 5 M NaCl up to final concentration 125 mM (hyperosmolar conditions). Then cells were incubated for extra 24 h. In order to monitor glycerolipid de novo synthesis, 3 h before harvesting cells, 2 μCi/ml of [U-^{14}C]-glycerol were added to the media. After labeling, cells were collected and counted, and total lipids were analyzed as described in 2.6. Results are expressed as pmol of [^{14}C-Gly]-Glycerolipids / 1 x 10^6 cells ± SEM.

2.6. Lipid extraction, separation and quantitation. Total lipids were extracted by Bligh and Dyer method [18]. Briefly, after treatments (see 2.2.) or treatments and labelling (see 2.5.), MDCK cells were collected and counted, and ~3 × 10^6 cells were suspended in 800 μl of phosphate-buffered saline (PBS) and mixed with 2 ml of methanol and 1 ml of chloroform, vortexed gently for 30 s, and incubated on ice for 15 min. To obtain two phases, 1 ml of chloroform and 1 ml of water were added, vortexed for 30 s and centrifuged at 800 g for 5 min. The lower organic phase containing total cell lipids was collected, dried under a nitrogen stream, and kept at -80°C for further analysis. Different lipid species were separated by thin layer chromatography (TLC). To do this, dried extracts were applied drop by drop onto a 1 cm lane of thin-layer silica gel chromatoplates (Merck) and developed in a solvent system containing a mixture of petroleum ether / hexane / ethylic ether / acetic acid (40:40:20:1, v/v) [7]. The different lipids were identified by comparison with the corresponding standards and the retention factors (Rfs): 0, 0.13 and 0.60 for glycerophospholipids (GP), glycerolipids-diglycerol (GL-DG) and glycerolipids-triglycerol (GL-TG), respectively. All the

solvents used were of analytical grade and purchased from Merck Argentina.

2.6. Subcellular fractionation. To evaluate the presence of XBP1s in nuclear compartment, MDCK cells were grown in a mixture containing DMEM/Ham's-F12 (1:1), 10 % FBS and 1 % antibiotic mixture. After reaching 70–80% confluence, cells were placed in low-serum medium (0.5% FBS) for 24 h and then, MDCK cells were incubated in commercial media (isosmolar condition) or in hyperosmolar media for 24 and 48 h. MDCK cells were collected and ~ 10×10^6 cells were placed in a cold hypotonic-lysis buffer (10 mM Hepes-KOH, pH=7.9, 1.5 mM $MgCl_2$, 10 mM KCl and 0.4 % Triton X-100), and mechanically disrupted by using a 20-gauche needle syringe. Then, a 10 X solution A, containing 2.5 M sucrose, 250 mM Tris-HCl pH=7.4, 30 mM $MgCl_2$, 20 mM EDTA, was added to each sample to reach a final concentration 0.25 M sucrose, 25 mM Tris-HCl pH=7.4, 3 mM $MgCl_2$, 2 mM EDTA. Samples were centrifuged at 860 *g* for 15 min and the resulting pellet was washed twice with 1 X solution A, and then resuspended in an adequate volume with 1 X solution A. Protein content was determined by Lowry et al. procedure [19] and then, prepared for western blot analysis.

2.7. Western blot analysis. After hyperosmolar treatment (see 2.1.) or hyperosmolar treatment followed by fractionation (see 2.6.), aliquots containing 50 µg of protein were incubated with 4 × Laemmli buffer at 100°C for 5 min. Then, proteins were resolved in a 12.5 % SDS-polyacrylamide (Thermofisher) gels and blotted to polyvinylidene difluoride membranes (PVDF) (GE Healthcare Life science) at 100 V for 40 min. Membranes were blocked with 5 % non-fat milk in Tris-buffer saline (TBS:100 mM Tris-HCl, pH=7.5, 1.5 M NaCl)-1 % Tween 20 solution (TBS-Tween) and incubated overnight at 4°C with primary antibodies: goat polyclonal XBP1 antibody, 1:200 (Santa Cruz Biotechnology) or rabbit polyclonal β-Tubulin antibody, 1:5000 (AbCam). According to the manufacturer information, anti-XBP1 antibody (Santa Cruz Biotechnology, XBP-1 R14, SC 32136) is suitable for detecting both unspliced- (XBP1u) and spliced- (XBP1s) forms of XBP1 protein. After washing, blots were incubated with secondary antibodies: rabbit anti-goat horseradish peroxidase (HRP)-conjugated (1:5000) or donkey anti-rabbit HRP-conjugated 1:6000 (GE Healthcare Life science). Bands were evidenced by means of ECL Plus Western blotting analysis system (GE Healthcare Life science). Bands densitometries were performed with Gel Analyzer 19.1 online-free software.

2.8. Microscopy. Cells were cultured in isosmolar or hyperosmolar media for 24 and 48 h in the

absence or in the presence of 20 μM 4μ8C (see 2.2.) on glass coverslips. After treatments, cells were fixed in 4 % paraformaldehyde (Sigma-Aldrich) prepared in PBS solution for 15 min and permeabilized with 0.5 % triton X-100 for 10 min. Then, samples were blocked with 3 % BSA (bovine serum albumin, Sigma-Aldrich) in PBS for 60 min. After blocking, cells were incubated overnight with primary goat polyclonal anti-XBP1 antibody (1:20, Santa Cruz Biotechnology, XBP-1 R14, SC 32136) at 4°C. According to the manufacturer information, this antibody is suitable for detecting both unspliced- (XBP1u) and spliced- (XBP1s) forms of XBP1 protein. Primary interaction was evidenced by incubating samples with a secondary donkey anti-goat Alexa Fluor® 488 conjugated antibody, 1:200 (Abcam); DNA was stained with 2.5 μM Hoechst 33258 (Sigma-Aldrich) in wet chamber for 60 min at room temperature. Then, samples were washed with PBS and mounted with a drop of Vectashield mounting medium (Vector Laboratories). To evaluate lipid droplets, after treatments, cells were fixed in 4 % paraformaldehyde prepared in PBS solution for 15 min and permeabilized with 0.5 % triton X-100 for 10 min. After washing, cells were incubated with 0.5 % oil red O (Sigma-Aldrich) in isopropanol for 5 min. Then, samples were exhaustively washed with tap water and PBS. DNA was stained with 2.5 μM Hoechst 33258 (Sigma-Aldrich). Next, samples were mounted with a drop of Vectashield mounting medium (Vector Laboratories). Fluorescence images were obtained with a Nikon Eclipse Ti (with an objective Plan apo VC 60×, 1.4 DIC 1/2) with acquisition software Micrometrics SE Premium (Accu-Scope). Images were processed using Image J.

2.9. Statistical analysis. The results were expressed as mean ± SEM. Data from controls and different treatments were analyzed by ANOVA, and significant differences were assessed by a posteriori Dunnet test ($P < 0.05$).

3. Results.

3.1 Hyperosmolarity induces UPR and XBP1 activation in MDCK cells. Cells subjected to hyperosmolarity activate numerous adaptive mechanisms during the first 24 h after osmotic challenge [2, 20]. These include the expression of osmoprotective genes such as membrane cotransporters, sodium/myo-inositol transporter (*smit*) [21] and sodium/chloride/betaine transporter (*bgt1*) [22], both needed for organic osmolytes transport to counterbalance the rise in intracellular ionic strength, and the expression of cyclooxygenase 2 (*cox2*) which is involved in survival mechanisms [23, 24]. According to these reports, figure 1A and B show that 12 h of treatment with hyperosmolar medium increased *bgt1* and, in a lesser extent, *smit* (*bgt1*- and *smit*-mRNA) levels in MDCK cells, and both became significantly higher respect to control value after 24 h of treatment. *cox2* (*cox2*-mRNA) expression was also regulated by hyperosmolarity but with a different pattern. During the first 12 h of treatment, *cox2* levels decreased; but after 24 h of incubation *cox2* expression clearly increased respect to isosmolar level. It is interesting to note that maximal *cox2* expression was found after 48 h of hyperosmolarity when both *bgt1* and *smit* levels were minimal; this observation might evidence a synchronized osmoprotective gene expression. To determine whether hyperosmotic-protein synthesis activation may induce ER stress, the expression of UPR markers, *xbp1*, *chop* and *bip/grp78*, were determined at the mRNA level. Figures 1C and D show that hyperosmolarity induced ER stress and UPR activation in MDCK cells. Hyperosmolar media increased *xbp1* and *chop* levels after 24 h and both remained elevated after 48 h. It is worth pointing out that the rise in UPR markers became evident after the increase of osmoprotective genes expression. In contrast, hyperosmolar treatment did not change *bip/grp78*-mRNA level at any experimental time assayed.

Triggering of Inositol-Requiring-Enzyme 1α (IRE1α)-UPR pathway involves the activation of IRE1α-endoribonuclease (RNase) activity which initiates a non-conventional mRNA splicing reaction of the pre-existing *xbp1* mRNA *(xbp1u*). As a result of IRE1α action, spliced-*xbp1* mRNA *(xbp1s*) increases. *xbp1s* translation yields XBP1s protein, a transcription factor that translocates to the nucleus and initiates the transcription of UPR-related and non-related genes, *xbp1* itself among them [10, 25]. In order to assess whether hyperosmolarity-increased *xbp1* expression (Fig. 1C) reflects its activation, we determined *xbp1u* and *xbp1s* forms, XBP1 protein and its presence in nuclear compartment (Fig. 2). To evaluate mRNA levels, we designed specific primers that detect both *xbp1u* and *xbp1s* (see

table 1 in Materials and Methods). Fig. 2 A shows *xbp1u* and *xbp1s* levels in isosmolar conditions (0 h incubation with hyperosmolar medium) and after 6, 12, 24 and 48 h of incubation in hyperosmolar medium. Figure 2 B shows the densitometric analysis of *xbp1* bands, each bar is a stacked representation of *xbp1u* and *xbp1s values (arbitrary units).* As it can be seen, in isosmolarity, most mRNA corresponded to *xbp1u* (70 ± 8 % vs. 30 ± 6%, *xbp1u* vs *xbp1s*, respectively). After 6 and 12 h of treatment with hyperosmolar medium, the levels of total *xbp1* decreased; however, the proportion of *xbp1s* after 6 and 12 h of treatment was higher than the proportion of *xbp1s* in isosmolar condition (41 ± 5 % and 39 ± 3 % vs. 30 ± 6%, after 6 and 12 h of treatment vs. isosmolar condition, respectively); 24 h of hyperosmolarity induced total *xbp1* expression (Fig. 1 C and D) and its splicing (Fig. 2 A and B). At that time, *xbp1s* represented 49 ± 5 % of total mRNA being significantly higher than isosmolar value (30 ± 6 %). The maximal *xbp1* levels were found after 48 h of treatment and the relative amounts of *xbp1u* and *xbp1s* were comparable to isosmolar values (69 ± 8 % and 31 ± 6 % for *xbp1u* and *xbp1s*, respectively). The last lane corresponds to the treatment with ER stress inducer tunicamycin (Tm). These results evidence the increase of IRE1α associated- endoribonuclease activity leading to the rise in *xbp1s* and confirm hyperosmolar-triggering of UPR. Figure 2 C shows XBP1 protein expression. When western blot analysis was performed from whole MDCK cell lysates, the only band detected corresponded to the 28 kDa XBP1u protein. The densitometric analysis showed a slight but significant increase of XBP1u as a function of the time, being maximal after 24 h of treatment (Fig. 2 C and D). However, we were not able to detect a 55 kDa band corresponding to the spliced form of the protein. Considering that antibody can detect both XBP1u and XBP1s proteins, we hypothesized that the loss of XBP1s band in western blot analysis could have been due to the low proportion of XBP1s form in whole lysate. We thought that the low levels of XBP1s could be detected if we analyzed nuclear compartment. To do that, we obtained nuclear fractions from isosmolar and hyperosmolar MDCK cultures by differential centrifugation and then, performed western blot analysis. As it is seen in figure 2 E, 24 h of hyperosmolarity increased XBP1 mature form in nuclear compartment, reaching a maximum after 48 h of treatment. The presence of XBP1s in nuclear compartment was also evidenced by fluorescence microscopy (Fig. 2 F). In isosmolar condition, most label was concentrated in cytoplasmic dots (Fig. 2 F) but 24 and 48 h of treatment caused the redistribution of the immunolabelling to the nuclear compartment (Fig. 2 F). Together, these results

demonstrate that hyperosmolarity induces ER stress, UPR and XBP1 activation.

3.2 XBP1 expression is required for osmotic activation of lipid synthesis. The ER is the major site of lipid metabolism as many enzymes involved in lipid synthesis reside in ER membranes [26]. Although the UPR activation was originally associated to maintain the protein homeostasis in the ER, a growing number of studies suggest that UPR plays essential roles in maintaining lipid metabolism and homeostasis [27]. We previously showed that hyperosmolarity upregulates phospholipid and triglycerides synthesis and content in renal cells [6, 7]; Fagone et al demonstrated that cell differentiation occurs with activation of membrane lipid synthesis which requires XBP1 activation [28]. Thus, we decided to evaluate whether hyperosmolarity-induced XBP1s (Fig. 2 E and F) was involved in glycerolipid metabolism in MDCK cells. To do that, two different strategies were used: the silencing of *xbp1*gene and the inhibition of the IRE1α activity by 4μ8C. As it was previously reported, hyperosmolarity increased glycerophospholipids (GP), triglycerides (GL-TG) and diglycerides (GL-DG) synthesis (Fig. 3 C and G). The treatment of cells with *xbp1*-siRNA, which reduced the expression of both *xbp1u* and *xbp1s* (Fig. 3A and B), significantly decreased hyperosmlarity-induced GL-TG synthesis (Fig. 3 C) as well as oil red-O staining (Fig. 3D). However, no changes were found neither in GP nor in GL-DG synthesis. The treatment of cells with 20 μM 4μ8C, that inhibits the RNAse activity of IRE1α, completely blocked the formation of *xbp1s*, in both isosmolar and hyperosmolar conditions (Figures 3E and F). As observed with *xbp1*-siRNA, 4μ8C considerably diminished GL-TG synthesis without changes in GP synthesis, but in this case, a slight but significant increase in GL-DG synthesis was observed (Fig. 3 G). Such a difference, compared with the synthesis of GL-DG in cells treated with *xbp1*-siRNA, may be due to the highest efficiency of 4μ8C in blocking the production of *xbp1s* (Fig. 3E vs. Fig. 3A). No changes were observed on lipid synthesis in isosmolar conditions by 4μ8C treatment. The decrease in GL-TG production was reflected in the reduction in the number (Fig. 3I) and in the size (Fig. 3J) of lipid droplets.

3.3. XBP1 regulates lipogenic genes expression. Hyperosmolar induction of GL-TG synthesis and accretion is associated to the transcriptional activation of main lipogenic enzymes such as LPIN1 and LPIN2, both involved in the conversion of phosphatidic acid into GL-DG; and DGAT1 and DGAT2 involved in the conversion of GL-DG into GL-TG [7]. As mentioned before, XBP1s transcription

factor can modulate the expression of different lipid metabolism enzymes [29, 30]. In addition, we found that the inhibition of *xbp1* synthesis or maturation dropped GL-TG synthesis (Fig. 3). Hence, we evaluated whether XBP1s regulates the transcription of *lpin1 and lpin2*, and *dgat1* and *dgat2 mRNAs*. To do that, MDCK cells were cultured for 24 h under hyperosmolar conditions in the absence or the presence of *xbp1*-siRNA (Fig.4 A and B) or 20 µM 4µ8C (Fig. 4 C and D). Both, *xbp1*-siRNA and 4µ8C decreased *lpin1, lpin2* and *dgat1* expression. However, no changes were observed for *dgat2* enzyme neither by using *xbp1*-siRNA nor by action of 4µ8C. We previously showed that hyperosmolarity increases the expression of the transcription factor *srebp* (Sterol Regulatory-Element Binding Protein) which mediates hyperosmolar induction of LPIN enzymes [7]. Thus, we evaluated the possibility that XBP1s was mediating *srebp* expression. As it is seen in figure 4, both *xbp1*-siRNA (Fig. 4 E and F) and RNAse inhibitor 4µ8C (Fig. 4 G and H) blocked the expression of *srebp1* and *srebp2* transcription factors. Together, these results indicate that XBP1s modulates lipogenic enzymes transcription by regulating the transcriptional activation of *srebp* transcription factor.

3.4. The role of TonEBP in hyperosmolar-induced XBP1 expression and activity. The transcription factor TonEBP (Tonicity Responsive-Enhancer Binding Protein) is considered the master regulator of osmoprotective response in renal cells. Its expression and translocation to the nucleus is rapidly activated by the increase of environmental osmolarity [2, 31, 32]. Once activated, TonEBP mediates the expression of osmoprotective proteins such as SMIT, BGT1 and COX2, among others. As XBP1 expression increased after 24 h of hyperosmolar treatment, we evaluated whether TonEBP activity was required for osmotic induction of XBP1. To do that, *tonebp*-siRNA was used to impede its expression. As it is shown in figure 5 A, *tonebp*-siRNA decreased *tonebp* mRNA as well as the levels of its target genes mRNAs: *smit* and *bgt1*. *tonebp* silencing also decreased the expression of hyperosmolar-induced *xbp1*-mRNA (Fig. 5 B and C), which in turn caused the fall in the expression of *srebps* mRNA (Fig. 5 D, E and F). Thus, hyperosmolar activation of TonEBP drives the transcriptional activation of *xbp1u* whose maturation, translation and activity are required for the regulation of lipid metabolism and homeostasis under hyperosmolar stress conditions.

4. Discussion.

The goal of the present work was to evaluate whether hyperosmolarity induces ER stress-UPR activation and the relationship between UPR and glycerolipid synthesis regulation in renal epithelial cells. The data presented herein demonstrate that hyperosmolarity activates IRE1α-XBP1 pathway (Fig. 1 and 2), and that XBP1 regulates glycerolipid synthesis through transcriptional regulation of the main lipogenic enzymes (Fig. 3 and 4) by means of XBP1-induced SREBP expression (Fig. 4). We also evidenced the relationship between TonEBP and XBP1 (Fig. 5).

Physiologically, renal medullary interstitium is characterized by its high osmolarity which is made of high and variable concentrations of urea and NaCl. Even more, environmental osmolarity may abruptly vary during urine concentration process [4]. To face up to the osmolar challenge cells activate the biosynthesis of various membrane-associated proteins such as the transporters sodium/myo-inositol transporter (SMIT), sodium/chloride/betaine transporter (BGT1), epithelial sodium channel (ENAC), urea transporter A and B (UTA and UTB), cystic fibrosis transmembrane conductance regulator (CFTR), Na^+/K^+-ATPase, glucose transporter 1 and 4 (GLUT1 and GLUT4), water channels (AQP1-5 and AQP9), metabolic enzymes (COX2) and receptors (AT1, type 1 angiotensin II receptor), among others [2, 21-24]. In addition, *in vivo* as well as *in vitro* experiments demonstrated that hyperosmolarity is a main signal for renal tubular cells differentiation and urinary concentrating mechanism maturation. During the first hours of hyperosmolar treatment, Madin-Darby Canine Kidney (MDCK) cells activates the expression of osmoprotective genes (Fig. 1 A and B). Once adapted, cells begin to execute a molecular program to achieve final polarized-differentiated phenotype that involves the increase in cell size and volume, and the formation of primary cilium [14]. Both processes involve a high rate of protein synthesis [2-4, 14]. Thus, it is logical to hypothesize that hyperosmolarity induces ER stress. Apart from unfolded proteins, IRE1α might sense lipid bilayer stress [33-35]. Thus, perturbations in ER-membranes by the excess of fatty acids (especially saturated fatty acids), either by de novo synthesis or by GL-TG hydrolysis, can directly activate IRE1α independently of unfolded proteins [34]. It has been reported that a feature of lipid-dependent activation of UPR is the absence of changes in the levels of BiP chaperone [34]. We previously demonstrated that hyperosmolarity increases *acc* and *fas* expression and *de novo* fatty acids synthesis [7]. Thus, it is possible that the rapid increase in saturated fatty acids affects ER membrane

physicochemical properties with the subsequent activation of IRE1α - XBP1 pathway. This possibility might explain the fact that BiP chaperone expression did not change with hyperosmolar treatment (Fig. 1 C and D). However, such hypothesis must be proven.

We demonstrated that hyperosmolar medium induces phospholipid synthesis activity and phospholipid mass accretion in MDCK cells within the first 48 h of hypertonic treatment. The upregulation of GP synthesis is needed for membrane biogenesis during cell polarization-differentiation processs, since it contributes to the enrichment of the apical and basolateral membranes in sphingomyelin (SM) and phosphatidylcholine (PC) content, respectively [6]. Here we show that XBP1s regulates lipogenic enzymes expression; thus, XBP1s participates in renal cell differentiation by activating lipid metabolism. XBP1 has been associated to eosinophils differentiation [36], adipose cell differentiation and myogenesis [37], cardiac myogenesis, hepatogenesis, plasma cell differentiation and development of secretory tissues [38, 39]. Despite it is known that XBP1 can direct the expression of diverse types of proteins [40], it is accepted that XBP1 promotes differentiation, at least in part, by regulating the biogenesis and expansion of organelles involved in secretion, including the ER and Golgi [41, 42]. Our results demonstrate that XBP1 directs the expression of lipogenic enzymes which are needed for membranes biogenesis in cell polarization and differentiation. In addition, we show that XBP1 expression is mediated by TonEBP (Fig. 5), which has also been involved in renal cell differentiation [1], skeletal muscle differentiation [43], P19CL6 cells differentiation to cardiomyocytes [44], CACO-2 cell differentiation [45] and human bone marrow stem cells (hBMSCs) differentiation to chondrogenic cells [46]. Therefore, we can hypothesize that high sodium environment induces MDCK cells differentiation by activating TonEBP transcription factor which, at least in part, regulates XBP1 expression. In addition, XBP1 would constitute an osmoprotective protein since it drives the expression of lipogenic enzymes triggering a specific lipid synthesis program necessary for ER expansion that would restore ER homeostasis before cell differentiation.

IRE1α/XBP1s pathway was identified as a critical regulator of hepatic lipid metabolism [13]; XBP1s has been implicated in transcriptional regulation of many lipogenic genes such as *scd1* and *acc* [30] and CDP-choline pathway [29]. Herein we show that *xbp1* silencing as well as the inhibition of IRE1α RNAse activity by 4μ8C that hinders *xbp1* maturation, decreased the expression of *lpin1* and

lpin2 (Fig. 4), both involved in the generation of GL-DG needed for PC, PE and GL-TG synthesis. GL-DG biosynthesis was not reduced by 4μ8C (Fig. 3), probably due to a remnant preexisting lipin activity. GL-DG seemed to be directed to GP more than to GL-TG synthesis, thus preserving membrane homeostasis. Impaired GL-TG production was probably due to the decrease in *dgat1* expression and the deviation of GL-DG substrate to GP synthesis. Previous report indicate that XBP1s regulates the expression of DGAT2 enzyme in hepatic tissue [13]; however, in our experimental conditions, *xbp1* maturation blockage did not decrease *dgat2* expression, but decreased *dgat1* (Fig. 4). Chitraju and coworkers demonstrated that both DGAT1 and DGAT2 contribute to GL-TG synthesis and storage in adipose tissue, and both can compensate for each other [47]. This is not the case in our system since *dgat2* is not impaired by XBP1 silencing or inhibition, but GL-TG synthesis is blocked; moreover, GL-DG was found significantly increased (Fig. 3).

It has been demonstrated that DGAT1, which is associated to ER membranes, has an exclusive role in protecting ER from the lipotoxic effect of an excess of fatty acids [48]. Considering our previous findings indicating that hyperosmolarity activates fatty acid synthesis [7], we can suggest that XBP1s contributes to ER homeostasis restoration and cell protection by activating the expression of *dgat1* that would clearance fatty acid excess. Hence, cells subjected to hyperosmolar stress hyperactivate ER-associated protein synthesis, that in turn activates the ER stress sensor IRE1α. This protein triggers *xbp1* maturation that conduce to the upregulation of fatty acid synthesis for membrane biogenesis; fatty acid excess is then cleaned up by LD formation. The increase in GP synthesis would, on one hand, provide new membrane extension to the jammed ER for carrying out the biosynthesis and maturation of osmoprotective proteins; the restoration of ER homeostasis would impede the activation of apoptotic or autophagic processes [49]. On the other hand, once ER functionality is restored, membrane biogenesis would be necessary for cell differentiation process, since glycerolipid, cholesterol and sphingolipid synthesis occur in ER membranes. Our data agree with previous reports showing the role of XBP1s in phosphatidylcholine synthesis, ER-membrane expansion and ER stress alleviation during B-lymphocyte differentiation [26, 28, 29].

One outstanding finding of our work was that *srebp* expression is mediated by XBP1s. We previously showed that hyperosmolarity upregulates glycerolipid synthesis due to an increase in the expression and activity of LPIN enzymes. Transcriptional activation of *lpin1* and *lpin2* expression is

mediated by SREBP [6-8]. Here we show for the first time that renal expression of *srebp1* and *srebp2* is mediated by XBP1s (Fig. 4). Our finding agrees with the only one previous report from Ning et al. showing that insulin-mediated hepatic lipogenesis involved IRE1α-XBP1s activation and *srebp1c* transcription upregulation [50].

Summarizing, in the present work we studied whether hyperosmolarity triggers ER-stress and UPR activation and its relationship with lipid synthesis in renal cells. Based on the present results we can hypothesize that the abrupt increase in the osmolarity of the environment induces signaling pathways that activate TonEBP transcription factor. TonEBP triggers the transcription of *smit, bgt1, cox2* and *xbp1* genes (among others). The products of these genes are membrane associated proteins whose synthesis occurs at endoplasmic reticulum (ER) membranes. The abrupt increase in ER-associated protein synthesis, causes ER stress and IRE1α activation. IRE1α-associated endoribonuclease splices *xbp1u* to *xbp1s*, which is translated to XBP1s protein. XBP1s translocates to the nucleus, binds to its response element in DNA and activates the transcription of *srebp* (among other genes). After its cytoplasmic translation, which also occurs at ER membranes, SREBP is activated, translocates to nuclear compartment and initiates the transcription of lipogenic genes: *dgat1, lpin1,* and *lpin2,* and as consequence, lipid synthesis is enhanced. The increase in glycerolipids content facilitates ER membranes expansion and alleviation of ER stress (Fig. 6). Therefore, XBP1 acts as an osmoprotective protein since it is activated by high osmolarity through TonEBP and it drives biomembranes generation and ER homeostasis restoration.

Conflict of interest

The authors declare that they have no conflicts of interest with the contents of this article.

Funding sources

This work was supported by Agencia Nacional de Promoción Científica y Tecnológica [grant: PICT 2013-1132], Consejo Nacional de Investigaciones Científicas y Tecnológicas (CONICET) [grant PIP0327], University of Buenos Aires [UBACYT 2014-2017, 20020130100658BA] and Escuelas ORT Argentina [2015-ORT Grant]

4. References

[1] K.H. Han, S.K. Woo, W.Y. Kim, S.H. Park, J.H. Cha, J. Kim, H.M. Kwon, Maturation of TonEBP expression in developing rat kidney, American journal of physiology. Renal physiology, 287 (2004) F878-885.

[2] M.B. Burg, J.D. Ferraris, N.I. Dmitrieva, Cellular response to hyperosmotic stresses, Physiological reviews, 87 (2007) 1441-1474.

[3] D. Kultz, Hypertonicity and TonEBP promote development of the renal concentrating system, American journal of physiology. Renal physiology, 287 (2004) F876-877.

[4] J.M. Sands, H.E. Layton, Advances in understanding the urine-concentrating mechanism, Annual review of physiology, 76 (2014) 387-409.

[5] J. Danziger, M.L. Zeidel, Osmotic homeostasis, Clinical journal of the American Society of Nephrology : CJASN, 10 (2015) 852-862.

[6] C.I. Casali, K. Weber, N.O. Favale, M.C. Tome, Environmental hyperosmolality regulates phospholipid biosynthesis in the renal epithelial cell line MDCK, J Lipid Res, 54 (2013) 677-691.

[7] K. Weber, C. Casali, V. Gaveglio, S. Pasquare, E. Morel Gomez, L. Parra, L. Erjavec, C. Perazzo, M.C. Fernandez Tome, TAG synthesis and storage under osmotic stress. A requirement for preserving membrane homeostasis in renal cells, Biochimica et biophysica acta. Molecular and cell biology of lipids, 1863 (2018) 1108-1120.

[8] N.O. Favale, M.C. Fernandez-Tome, L.G. Pescio, N.B. Sterin-Speziale, The rate-limiting enzyme in phosphatidylcholine synthesis is associated with nuclear speckles under stress conditions, Biochim Biophys Acta, 1801 (2010) 1184-1194.

[9] D.S. Schwarz, M.D. Blower, The endoplasmic reticulum: structure, function and response to cellular signaling, Cell Mol Life Sci, 73 (2016) 79-94.

[10] R. Bravo, V. Parra, D. Gatica, A.E. Rodriguez, N. Torrealba, F. Paredes, Z.V. Wang, A. Zorzano, J.A. Hill, E. Jaimovich, A.F. Quest, S. Lavandero, Endoplasmic reticulum and the unfolded protein response: dynamics and metabolic integration, Int Rev Cell Mol Biol, 301 (2013) 215-290.

[11] C. Hetz, The unfolded protein response: controlling cell fate decisions under ER stress and beyond, Nat Rev Mol Cell Biol, 13 (2012) 89-102.

[12] L.H. Glimcher, XBP1: the last two decades, Ann Rheum Dis, 69 Suppl 1 (2010) i67-71.

[13] A.H. Lee, E.F. Scapa, D.E. Cohen, L.H. Glimcher, Regulation of hepatic lipogenesis by the transcription factor XBP1, Science, 320 (2008) 1492-1496.

[14] L.G. Pescio, N.O. Favale, M.G. Marquez, N.B. Sterin-Speziale, Glycosphingolipid synthesis is essential for MDCK cell differentiation, Biochim Biophys Acta, 1821 (2012) 884-894.

[15] W. Strober, Trypan Blue Exclusion Test of Cell Viability, Current protocols in immunology, 111 (2015) A3 B 1-A3 B 3.

[16] B.C. Cross, P.J. Bond, P.G. Sadowski, B.K. Jha, J. Zak, J.M. Goodman, R.H. Silverman, T.A. Neubert, I.R. Baxendale, D. Ron, H.P. Harding, The molecular basis for selective inhibition of unconventional mRNA splicing by an IRE1-binding small molecule, Proc Natl Acad Sci U S A, 109 (2012) E869-878.

[17] K.Y. Na, S.K. Woo, S.D. Lee, H.M. Kwon, Silencing of TonEBP/NFAT5 transcriptional activator by RNA interference, Journal of the American Society of Nephrology : JASN, 14 (2003) 283-288.

[18] E.G. Bligh, W.J. Dyer, A rapid method of total lipid extraction and purification, Can J Biochem Physiol, 37 (1959) 911-917.

[19] O.H. Lowry, N.J. Rosebrough, A.L. Farr, R.J. Randall, Protein measurement with the Folin phenol reagent, J Biol Chem, 193 (1951) 265-275.

[20] R.R. Alfieri, P.G. Petronini, Hyperosmotic stress response: comparison with other cellular stresses, Pflugers Arch, 454 (2007) 173-185.

[21] A. Yamauchi, H.M. Kwon, S. Uchida, A.S. Preston, J.S. Handler, Myo-inositol and betaine transporters regulated by tonicity are basolateral in MDCK cells, Am J Physiol, 261 (1991) F197-202.

[22] H. Miyakawa, J.S. Rim, J.S. Handler, H.M. Kwon, Identification of the second tonicity-responsive enhancer for the betaine transporter (BGT1) gene, Biochim Biophys Acta, 1446 (1999) 359-364.

[23] N.O. Favale, C.I. Casali, L.G. Lepera, L.G. Pescio, M.C. Fernandez-Tome, Hypertonic induction of COX2 expression requires TonEBP/NFAT5 in renal epithelial cells, Biochem Biophys Res Commun, 381 (2009) 301-305.

[24] T. Yang, I. Singh, H. Pham, D. Sun, A. Smart, J.B. Schnermann, J.P. Briggs, Regulation of cyclooxygenase expression in the kidney by dietary salt intake, Am J Physiol, 274 (1998) F481-489.

[25] S. Fu, S.M. Watkins, G.S. Hotamisligil, The role of endoplasmic reticulum in hepatic lipid homeostasis and stress signaling, Cell Metab, 15 (2012) 623-634.

[26] P. Fagone, S. Jackowski, Membrane phospholipid synthesis and endoplasmic reticulum function, J Lipid Res, 50 Suppl (2009) S311-316.

[27] J. Han, R.J. Kaufman, The role of ER stress in lipid metabolism and lipotoxicity, J Lipid Res, 57 (2016) 1329-1338.

[28] P. Fagone, R. Sriburi, C. Ward-Chapman, M. Frank, J. Wang, C. Gunter, J.W. Brewer, S. Jackowski, Phospholipid biosynthesis program underlying membrane expansion during B-lymphocyte differentiation, J Biol Chem, 282 (2007) 7591-7605.

[29] R. Sriburi, S. Jackowski, K. Mori, J.W. Brewer, XBP1: a link between the unfolded protein response, lipid biosynthesis, and biogenesis of the endoplasmic reticulum, The Journal of cell biology, 167 (2004) 35-41.

[30] C. Piperi, C. Adamopoulos, A.G. Papavassiliou, XBP1: A Pivotal Transcriptional Regulator of Glucose and Lipid Metabolism, Trends Endocrinol Metab, 27 (2016) 119-122.

[31] S.N. Ho, The role of NFAT5/TonEBP in establishing an optimal intracellular environment, Arch Biochem Biophys, 413 (2003) 151-157.

[32] S.K. Woo, S.D. Lee, H.M. Kwon, TonEBP transcriptional activator in the cellular response to increased osmolality, Pflugers Arch, 444 (2002) 579-585.

[33] K. Halbleib, K. Pesek, R. Covino, H.F. Hofbauer, D. Wunnicke, I. Hanelt, G. Hummer, R. Ernst, Activation of the Unfolded Protein Response by Lipid Bilayer Stress, Molecular cell, 67 (2017) 673-684 e678.

[34] R. Volmer, K. van der Ploeg, D. Ron, Membrane lipid saturation activates endoplasmic reticulum unfolded protein response transducers through their transmembrane domains, Proc Natl Acad Sci U S A, 110 (2013) 4628-4633.

[35] N.S. Hou, S. Taubert, Membrane lipids and the endoplasmic reticulum unfolded protein response: An interesting relationship, Worm, 3 (2014) e962405.

[36] S.E. Bettigole, R. Lis, S. Adoro, A.H. Lee, L.A. Spencer, P.F. Weller, L.H. Glimcher, The transcription factor XBP1 is selectively required for eosinophil differentiation, Nat Immunol, 16 (2015) 829-837.

[37] Y. He, S. Sun, H. Sha, Z. Liu, L. Yang, Z. Xue, H. Chen, L. Qi, Emerging roles for XBP1, a sUPeR transcription factor, Gene Expr, 15 (2010) 13-25.

[38] A.H. Lee, G.C. Chu, N.N. Iwakoshi, L.H. Glimcher, XBP-1 is required for biogenesis of cellular secretory machinery of exocrine glands, EMBO J, 24 (2005) 4368-4380.

[39] A.M. Reimold, N.N. Iwakoshi, J. Manis, P. Vallabhajosyula, E. Szomolanyi-Tsuda, E.M. Gravallese, D. Friend, M.J. Grusby, F. Alt, L.H. Glimcher, Plasma cell differentiation requires the transcription factor XBP-1, Nature, 412 (2001) 300-307.

[40] D. Acosta-Alvear, Y. Zhou, A. Blais, M. Tsikitis, N.H. Lents, C. Arias, C.J. Lennon, Y. Kluger, B.D. Dynlacht, XBP1 controls diverse cell type- and condition-specific transcriptional regulatory networks, Molecular cell, 27 (2007) 53-66.

[41] A.L. Shaffer, M. Shapiro-Shelef, N.N. Iwakoshi, A.H. Lee, S.B. Qian, H. Zhao, X. Yu, L. Yang, B.K. Tan, A. Rosenwald, E.M. Hurt, E. Petroulakis, N. Sonenberg, J.W. Yewdell, K. Calame, L.H. Glimcher, L.M. Staudt, XBP1, downstream of Blimp-1, expands the secretory apparatus and other organelles, and increases protein synthesis in plasma cell differentiation, Immunity, 21 (2004) 81-93.

[42] R. Sriburi, H. Bommiasamy, G.L. Buldak, G.R. Robbins, M. Frank, S. Jackowski, J.W. Brewer, Coordinate regulation of phospholipid biosynthesis and secretory pathway gene expression in XBP-1(S)-induced endoplasmic reticulum biogenesis, J Biol Chem, 282 (2007) 7024-7034.

[43] R.S. O'Connor, G.K. Pavlath, Point:Counterpoint: Satellite cell addition is/is not obligatory for skeletal muscle hypertrophy, J Appl Physiol (1985), 103 (2007) 1099-1100.

[44] A. Adachi, T. Takahashi, T. Ogata, H. Imoto-Tsubakimoto, N. Nakanishi, T. Ueyama, H. Matsubara, NFAT5 regulates the canonical Wnt pathway and is required for cardiomyogenic differentiation, Biochem Biophys Res Commun, 426 (2012) 317-323.

[45] Q. Wang, Y. Zhou, P. Rychahou, C. Liu, H.L. Weiss, B.M. Evers, NFAT5 represses canonical Wnt signaling via inhibition of beta-catenin acetylation and participates in regulating intestinal cell differentiation, Cell death & disease, 4 (2013) e671.

[46] M.M. Caron, A.E. van der Windt, P.J. Emans, L.W. van Rhijn, H. Jahr, T.J. Welting, Osmolarity determines the in vitro chondrogenic differentiation capacity of progenitor cells via nuclear factor of activated T-cells 5, Bone, 53 (2013) 94-102.

[47] C. Chitraju, T.C. Walther, R.V. Farese, Jr., The triglyceride synthesis enzymes DGAT1 and

DGAT2 have distinct and overlapping functions in adipocytes, J Lipid Res, 60 (2019) 1112-1120.

[48] C. Chitraju, N. Mejhert, J.T. Haas, L.G. Diaz-Ramirez, C.A. Grueter, J.E. Imbriglio, S. Pinto, S.K. Koliwad, T.C. Walther, R.V. Farese, Jr., Triglyceride Synthesis by DGAT1 Protects Adipocytes from Lipid-Induced ER Stress during Lipolysis, Cell Metab, 26 (2017) 407-418 e403.

[49] A.V. Cybulsky, Endoplasmic reticulum stress, the unfolded protein response and autophagy in kidney diseases, Nat Rev Nephrol, 13 (2017) 681-696.

[50] J. Ning, T. Hong, A. Ward, J. Pi, Z. Liu, H.Y. Liu, W. Cao, Constitutive role for IRE1alpha-XBP1 signaling pathway in the insulin-mediated hepatic lipogenic program, Endocrinology, 152 (2011) 2247-2255.

Figure Legends

Figure 1. Hyperosmolarity induces changes in osmoprotective- and UPR markers-mRNA levels. MDCK cells were grown in a mixture containing DMEM/Ham's-F12 (1:1), 10 % FBS and 1 % antibiotic mixture. After reaching 70–80% confluence, cells were placed in low serum medium (0.5% FBS) and incubated in isosmolar media (commercial media, 298 ± 19 mOsmol/Kg of water, no addition of NaCl) or in hyperosmolar media (commercial media added with sterile 5 M NaCl up to 512 ± 12 mOsm/Kg of water) for 6, 12, 24 and 48 h. After treatments, cells were collected, counted and subjected to RNA extraction as described in Methods. Both osmoprotective genes (*cox2*, *smit* and *bgt-1*) (A), and UPR activation markers (*xbp1, chop* and *bip*) (C) mRNA levels were evaluated by RT-PCR. The images correspond to a representative experiment from three independent determinations. Bar graphs, B and D correspond to the densitometric analysis of the bands performed with GelAnalizer 19.1 online software. They represent the ratio between the values of each mRNA and *β-actin* (arbitrary units) and express the mean ± SEM of three independent experiments. Significant differences are shown within bar graphs.

Figure 2. Hyperosmolarity induces XBP1 activation. Panel A: MDCK cells were grown in a mixture containing DMEM/Ham's-F12 (1:1), 10% FBS and 1% antibiotic mixture. After reaching 70–80% confluence, cells were placed in low serum medium (0.5% FBS) and incubated in isosmolar media (commercial media, 298 mOsmol/Kg of water, 0 h of NaCl) or in hyperosmolar media (commercial media added with sterile 5 M NaCl up to 512 mOsm/Kg of water) for 6, 12, 24 and 48 h. In order to assess whether IRE1α - XBP1 pathway was active, specific primers were designed (Table 1, Methods) to detect unspliced- (immature) and spliced- (mature) forms of *xbp1* mRNA (*xbp1u* and *xbp1s*) by RT-PCR. Tunicamycin (Tm) was used as a positive control of pathway activation.

Panel B shows densitometric analysis of the gel shown in A. Each bar is a stacked representation of *xbp1u* and *xbp1s values*. Densitometric analysis of the bands was performed with Gel Analizer 19.1 online software and represent the ratio between the values of *xbp1u* or *xbp1s* and β-actin (arbitrary units). Each bar represents the mean ± SEM of three independent experiments.

Panel C shows a representative image of three independent western blot analysis of XBP1u protein and panel D shows the densitometric analysis of bands. Each bar represents the mean ± SEM of the

ratio between XBP1u and β-Tubulin (arbitrary units). Although the antibody used (goat polyclonal anti-XBP1 antibody, 1:200, Santa Cruz Biotechnology, XBP-1 R14, SC 32136) is reported to detect both XBP1 isoforms under our experimental conditions, XBP1s band (~55kDa) was not evidenced, probably due to the low proportion of this protein in total lysates. Then, western blot analysis was performed in nuclear fractions obtained by cell fractionation.

Panel E shows a representative image of cell fractionation followed by western blot analysis of XBP1. For this experiment, MDCK cells were grown in a mixture containing DMEM/Ham's-F12 (1:1), 10% FBS and 1% antibiotic mixture. After reaching 70–80% confluence, cells were placed in low serum medium (0.5% FBS) and incubated in isosmolar media (commercial media, 298 mOsmol/Kg of water, 0 h of NaCl) or in hyperosmolar media (commercial media added with sterile 5 M NaCl up to 512 mOsm/Kg of water) for 24 and 48 h. After treatment MDCK cells were collected and ~ 10×10^6 cells were placed in a cold hypotonic-lysis buffer (10 mM Hepes-KOH, pH=7.9, 1.5 mM $MgCl_2$, 10 mM KCl and 0.4 % Triton X-100), and mechanically disrupted by using a 20-gauche needle syringe. Then, a 10 X solution A, containing 2.5 M sucrose, 250 mM Tris-HCl pH=7.4, 30 mM $MgCl_2$, 20 mM EDTA was added to each sample to reach a final concentration 0.25 M sucrose, 25 mM Tris-HCl pH=7.4, 3 mM $MgCl_2$, 2 mM EDTA. Samples were centrifuged at 860 *g* for 15 min and the resulting pellet was washed twice with 1 X solution A, and then resuspended in an adequate volume for western blot analysis.

Panel F shows the distribution of XBP1 protein by fluorescence microscopy. For this experiment, cells were grown on coverslips and after treatments (described in Materials and Methods), cells were fixed with 4% paraformaldehyde in PBS followed by 0.5 % triton X-100 permeabilization. Immunodetection was performed with goat polyclonal anti-XBP1 antibody (1:20, Santa Cruz Biotechnology, XBP-1 R14, SC 32136) that can detect both XBP1 isoforms. Primary interaction was evidenced by incubating samples with a secondary donkey anti-goat Alexa Fluor® 488 conjugated antibody, 1:200 (Abcam) and 2.5 μM Hoechst. Samples were mounted with a drop of Vectashield mounting medium (Vector Laboratories). Images were processed with Image J and are representative of three independent experiments. Where applicable, significances were included within the graphs.

Figure 3. The role of XBP1 in lipid metabolism. Panel A: MDCK cells were grown in a mixture containing DMEM/Ham's-F12 (1:1), 10% FBS and 1% antibiotic mixture. After reaching 70–80% confluence, cells were placed in low serum medium (0.5% FBS) and then transfected with *xbp1*-siRNA. After 24 h cells were subjected to hyperosmolar medium for extra 24 h. After treatment, cells were harvested, RNA was isolated and *xbp1* mRNA was evaluated by RT-PCR analysis.

Panel B shows the densitometric analysis of gel shown in panel A. Densitometric analysis of the bands was performed with Gel Analizer 19.1 online software and each bar represents the ratio between the values of *xbp1u* or *xbp1s* and *β-actin* (arbitrary units). Each bar represents the mean ± SEM of three independent experiments. Significative results are indicated within the graph.

Panel C: To analyze the role of XBP1 in lipid metabolism, MDCK cells were grown in a mixture containing DMEM/Ham's-F12 (1:1), 10% FBS and 1% antibiotic mixture. After reaching 70–80% confluence, cells were placed in low serum medium (0.5% FBS) and then transfected with with *xbp1*-siRNA. After 24 h cells were subjected to hyperosmolar medium for extra 24 h; 3 h before harvesting 2 μCi/ml [U-^{14}C]-glycerol was added to each well. After labeling, cells were collected, and lipids were analyzed as described in Methods. The radioactivity incorporated to each lipid was visualized by radioautography and quantified by liquid scintillation counting. The results are expressed as pmol of [^{14}C-Gly]-glycerolipid/10^6 cells for GP, GL-TG and GL-DG and represent the mean ± SEM of four independent experiments.

Panel D: In addition, MDCK cells were grown on glass coverslips; after reaching 70–80% confluence, cells were placed in low serum medium (0.5% FBS) and then transfected with *xbp1*-siRNA. After 24 h cells were subjected to hyperosmolar medium for extra 24 h; after treatment, cells were fixed in 4 % paraformaldehyde in PBS solution and permeabilized with 0.5 % triton X-100. After washing, cells were incubated with 0.5 % oil red O in isopropanol; then, samples were exhaustively washed with tap water and PBS. Finally, samples were mounted in the presence of 2.5 μM Hoechst 33258 (Sigma-Aldrich) with a drop of Vectashield mounting medium (Vector Laboratories). Fluorescence images were obtained with a Nikon Eclipse Ti (with an objective Plan apo VC 60×, 1.4 DIC 1/2) with acquisition software Micrometrics SE Premium (Accu-Scope). Images were processed using Image J and are representative of three independent experiments.

Panel E: In other set of experiments, MDCK cells were grown in a mixture containing DMEM/Ham's-

F12 (1:1), 10% FBS and 1% antibiotic mixture. After reaching 70–80% confluence, cells were placed in low serum medium (0.5% FBS) and both, isosmolar and hyperosmolar cultures were treated with 20 µM 4µ8C, IRE1-XBP1 pathway inhibitor, for 30 min. Then cells were subjected to hyperosmolar medium for extra 24 h. After treatments, cells were harvested, RNA was isolated and *xbp1* mRNA was evaluated by RT-PCR analysis.

Panel F shows the densitometric analysis of gel shown in panel E which was performed with Gel Analizer 19.1 online software and each bar represents the ratio between the values of *xbp1u* or *xbp1s* and *β-actin* (arbitrary units). Each bar represents the mean ± SEM of three independent experiments. Significative results are indicated within the graph.

Panel G: To analyze the role of XBP1 in lipid metabolism, MDCK cells were grown in a mixture containing DMEM/Ham's-F12 (1:1), 10% FBS and 1% antibiotic mixture. After reaching 70–80% confluence, cells were placed in low serum medium (0.5% FBS) and both, isosmolar and hyperosmolar cells were treated with 20 µM 4µ8C for 30 min before NaCl addition; 3 h before harvesting 2 µCi/ml [U-^{14}C]-glycerol was added to each well. After labeling cells were collected and lipids were analyzed as described in Methods. The radioactivity incorporated to each lipid was visualized by radioautography and quantified by liquid scintillation counting. The results are expressed as pmol of [^{14}C-Gly]-glycerolipid/10^6 cells for GP, GL-TG and GL-DG and represent the mean ± SEM of four independent experiments.

Panel H. In addition, MDCK cells were grown on glass coverslips; after reaching 70–80% confluence, cells were placed in low serum medium (0.5% FBS) and both, isosmolar and hyperosmolar cultures were treated with 20 µM 4µ8C, IRE1-XBP1 pathway inhibitor, for 30 min. Then cells were subjected to hyperosmolar medium for extra 24 h. After treatments, cells were fixed in 4 % paraformaldehyde in PBS solution and permeabilized with 0.5 % triton X-100. After washing, cells were incubated with 0.5 % oil red O in isopropanol; then, samples were exhaustively washed with tap water and PBS. Finally, samples were mounted in the presence of 2.5 µM Hoechst 33258 with a drop of Vectashield mounting medium (Vector Laboratories). Fluorescence images were obtained with a Nikon Eclipse Ti (with an objective Plan apo VC 60×, 1.4 DIC 1/2) with acquisition software Micrometrics SE Premium (Accu-Scope). Images were processed using Image J and are representative of three independent experiments.

Panels I and J shows the quantification of the number and the size of lipid droplets showed in Panel H. Estimations were performed with Image J. Statistical significance is shown in each panel.

Figure 4. Lipid metabolism protein expression requires XBP1s activity. MDCK cells were grown in a mixture containing DMEM/Ham's-F12 (1:1), 10% FBS and 1% antibiotic mixture. After reaching 70–80% confluence, cells were placed in low serum medium (0.5% FBS) and then either transfected with *xbp1*-siRNA for 24 h, to knock down *xbp1* (panels A, B, E and F), or treated with 20 µM 4µ8C, an IRE1-XBP1 pathway inhibitor for 30 min (panels C, D, G and H). Then, cells were incubated in isosmolar media (commercial media, 298 mOsmol/Kg of water, no addition of NaCl) or in hyperosmolar media (commercial media added with sterile 5 M NaCl up to 512 mOsm/Kg of water) for 24 h. After treatments, cells were harvested, and RNA was isolated for RT-PCR analysis. *lpin 1*, *lpin2*, *dgat1* and *dgat2* mRNA expression in the presence of *xbp1*-siRNA (Panel A) and in the presence of IRE-XBP1 pathway inhibitor (Panel C) were evaluated. *srebp1* and *srebp2* mRNA expression in the presence of *xbp1*-siRNA (panel E) and in the presence of IRE-XBP1 pathway inhibitor (Panel G) were evaluated. The images correspond to a representative experiment from three independent determinations. Bar graphs in panels B, D, F and H correspond to the densitometric analysis of the bands performed with Gel Analizer 19.1 online software. Each bar represents the ratio between the values of each mRNA and *β-actin* (arbitrary units) and expresses the mean ± SEM of three independent experiments. Significant differences are shown within bar graphs.

Figure 5. TonEBP is involved in *xbp1*-mRNA expression. MDCK cells were grown in a mixture containing DMEM/Ham's-F12 (1:1), 10% FBS and 1% antibiotic mixture. After reaching 70–80% confluence, cells were placed in low serum medium (0.5% FBS) and then transfected with *tonebp*-siRNA to silence *tonebp* gene. After 24 h, cells were incubated in isosmolar media (commercial media, 298 mOsmol/Kg of water, no addition of NaCl) or in hyperosmolar media (commercial media added with sterile 5 M NaCl up to 512 mOsm/Kg of water) for extra 24 h. After treatment, cells were harvested and RNA was isolated and followed by RT-PCR to evaluate mRNA expression of *tonebp* and its target genes *smit* and *bgt1* (Panel A), *xbp1* (Panel B) and *srebp1* and *srebp2* (Panel D). The images correspond to a representative experiment from three independent determinations. Bar graphs in panels C, E, and F correspond to the densitometric analysis of the bands performed with Gel

Analizer 19.1 online software. Each bar represents the ratio between the values of each mRNA and *β-actin* (arbitrary units) and expresses the mean ± SEM of three independent experiments. Significant differences are shown within bar graphs.

Figure 6. The role of XBP1 in osmoprotection. Changes in environmental osmolarity induce signaling pathways that activate TonEBP transcription factor leading to the transcription of *smit, bgt1, cox2* and *xbp1* genes. These are membrane-associated proteins whose synthesis occurs at endoplasmic reticulum (ER) membranes. The increase in ER-associated protein synthesis causes ER stress and IRE1α activation. IRE1α-associated endoribonuclease splices *xbp1u* to *xbp1s,* which is translated to XBP1s. XBP1s translocates to the nucleus, binds to its response element (ERSE) in DNA and activates *srebp* transcription. The activation of SREBP, which is an ER membrane-associated protein, causes SREBP translocation to nuclear compartment and transcriptional activation of lipogenic genes: *dgat1, lpin1,* and *lpin2.* As consequence, lipid synthesis is enhanced, membrane expansion is facilitated, and ER stress alleviation occurs.

Highlights

- **XBP1 activity is modulated by hyperosmolarity.**
- **XBP1 expression is regulated by TonEBP, a hyperosmolar-induced transcription factor.**
- **XBP1 is involved in lipid synthesis through lipogenic genes upregulation.**
- **XBP1 would act as an osmoprotective protein.**

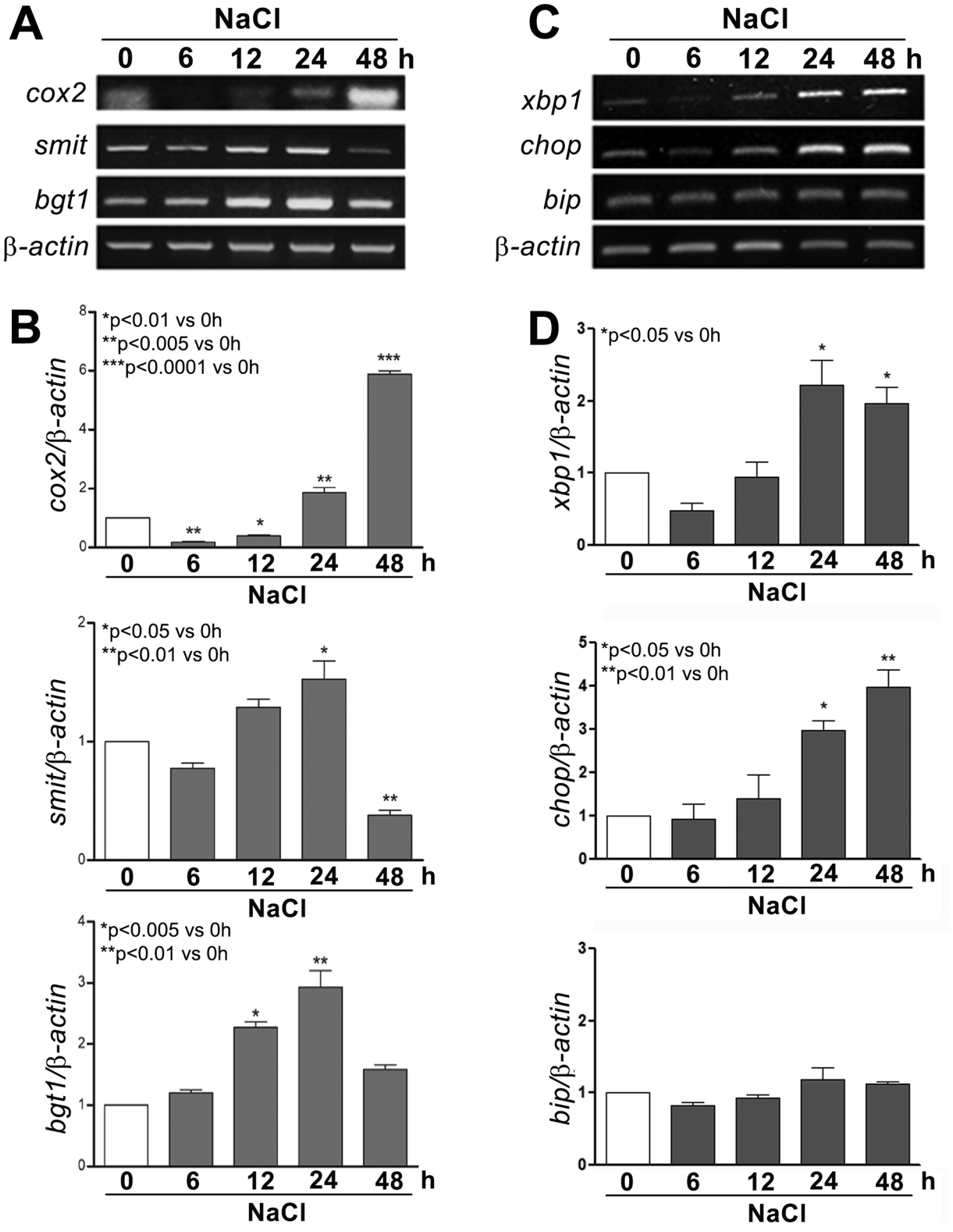
A
NaCl
0 6 12 24 48 h
cox2
smit
bgt1
β-actin
C
NaCl
0 6 12 24 48 h
xbp1
chop
bip
β-actin
B
*p<0.01 vs 0h
**p<0.005 vs 0h
***p<0.0001 vs 0h
cox2/β-actin
0 6 12 24 48 h
NaCl
*p<0.05 vs 0h
**p<0.01 vs 0h
smit/β-actin
0 6 12 24 48 h
NaCl
*p<0.005 vs 0h
**p<0.01 vs 0h
bgt1/β-actin
0 6 12 24 48 h
NaCl
D
*p<0.05 vs 0h
xbp1/β-actin
0 6 12 24 48 h
NaCl
*p<0.05 vs 0h
**p<0.01 vs 0h
chop/β-actin
0 6 12 24 48 h
NaCl
bip/β-actin
0 6 12 24 48 h
NaCl

Figure 1

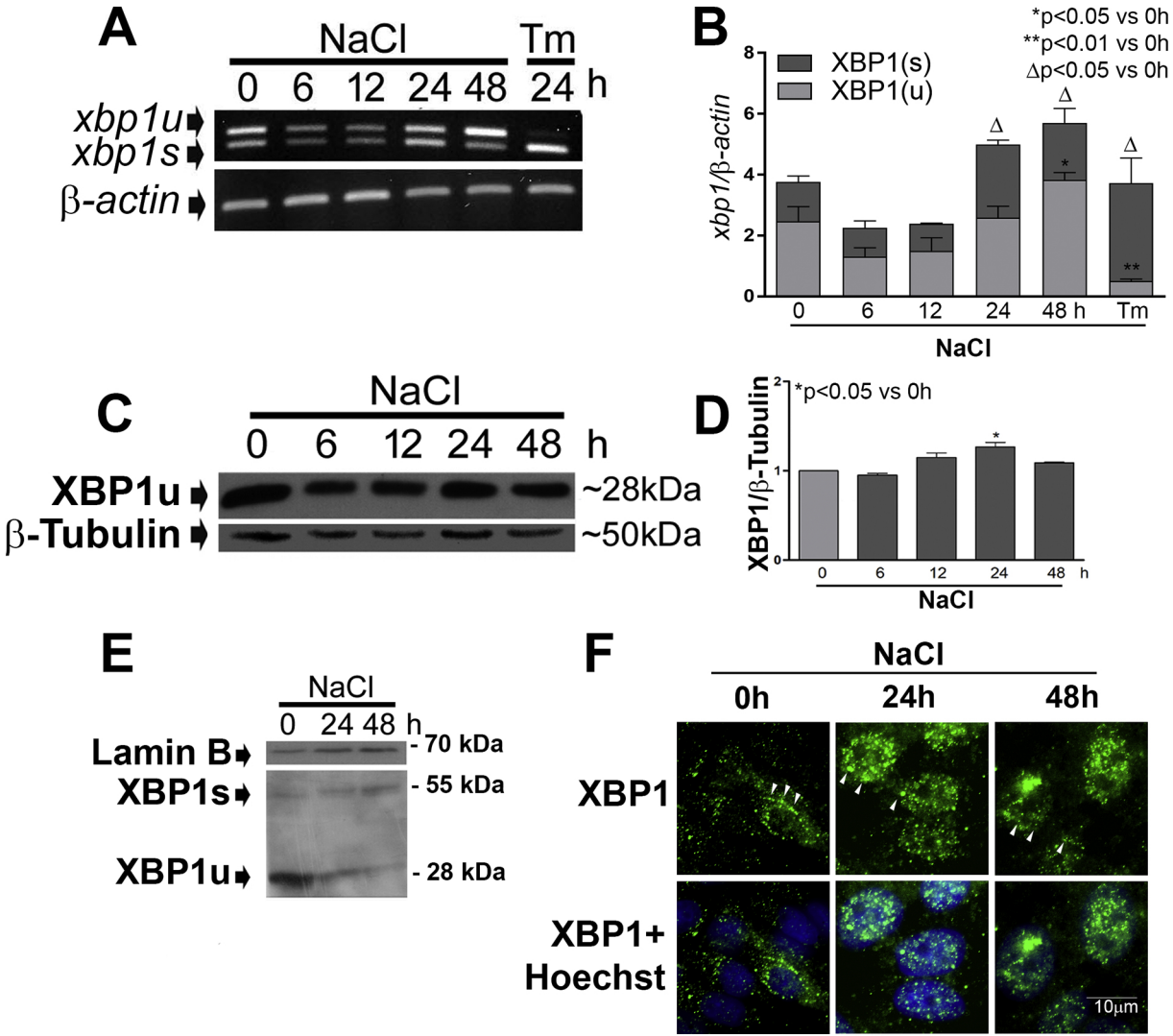
A
NaCl
Tm
0 6 12 24 48 24 h
xbp1u
xbp1s
β-actin
B
*p<0.05 vs 0h
**p<0.01 vs 0h
Δp<0.05 vs 0h
XBP1(s)
XBP1(u)
xbp1/β-actin
0 6 12 24 48 h Tm
NaCl
C
NaCl
0 6 12 24 48 h
XBP1u
β-Tubulin
~28kDa
~50kDa
D
*p<0.05 vs 0h
XBP1/β-Tubulin
0 6 12 24 48 h
NaCl
E
NaCl
0 24 48 h
Lamin B
XBP1s
XBP1u
- 70 kDa
- 55 kDa
- 28 kDa
F
NaCl
0h 24h 48h
XBP1
XBP1+
Hoechst
10μm

Figure 2

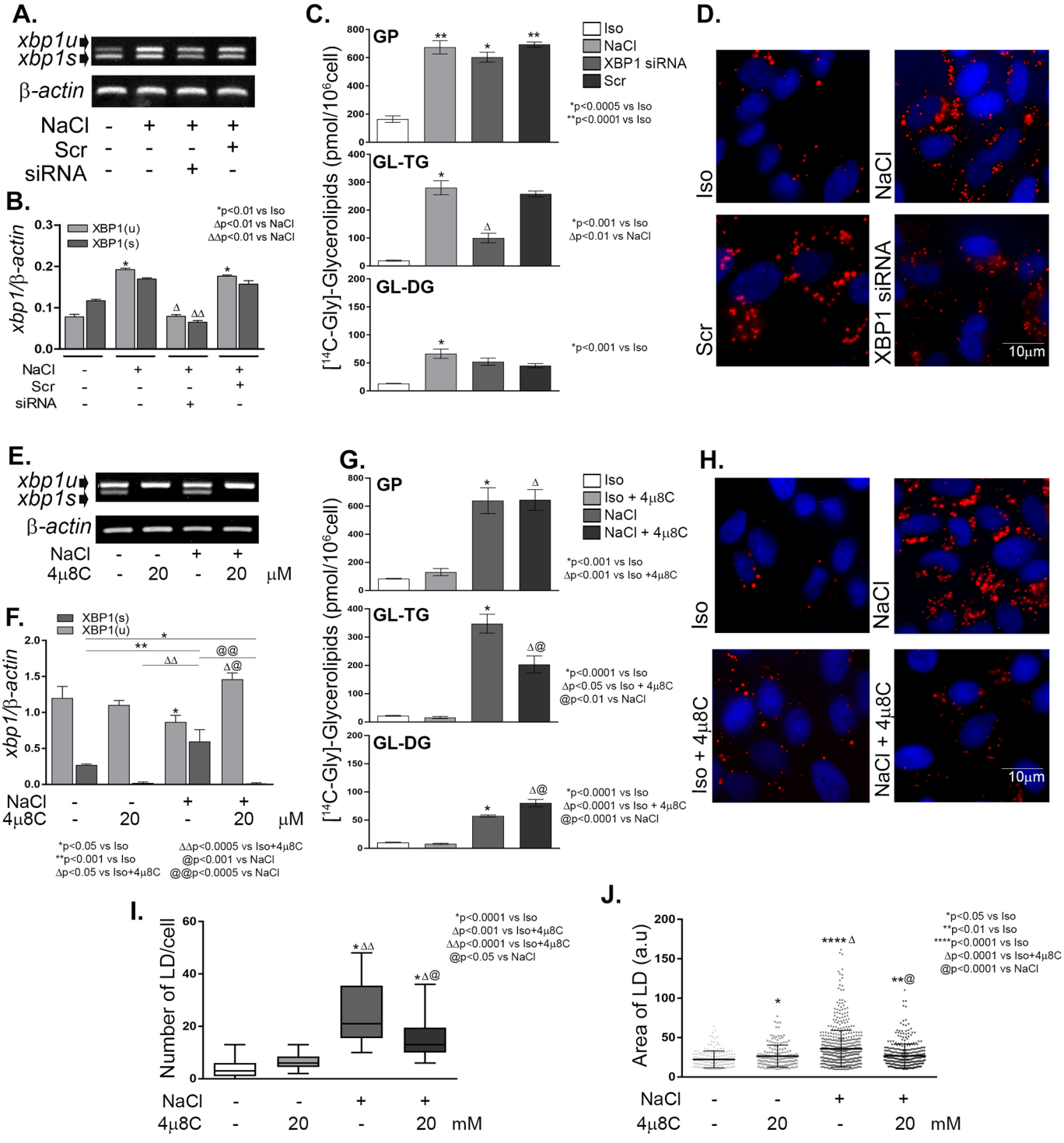
A.
xbp1u
xbp1s
β-actin
NaCl - + + +
Scr - - - +
siRNA - - + -
B.
*p<0.01 vs Iso
Δp<0.01 vs NaCl
ΔΔp<0.01 vs NaCl
XBP1(u)
XBP1(s)
xbp1/β-actin
NaCl - + + +
Scr - - - +
siRNA - - + -
C.
GP
GL-TG
GL-DG
[14C-Gly]-Glycerolipids (pmol/10^6cell)
Iso
NaCl
XBP1 siRNA
Scr
*p<0.0005 vs Iso
**p<0.0001 vs Iso
*p<0.001 vs Iso
Δp<0.01 vs NaCl
*p<0.001 vs Iso
D.
Iso
NaCl
Scr
XBP1 siRNA
10μm
E.
xbp1u
xbp1s
β-actin
NaCl - - + +
4μ8C - 20 - 20 μM
F.
XBP1(s)
XBP1(u)
xbp1/β-actin
NaCl - - + +
4μ8C - 20 - 20 μM
*p<0.05 vs Iso
**p<0.001 vs Iso
Δp<0.05 vs Iso+4μ8C
ΔΔp<0.0005 vs Iso+4μ8C
@p<0.001 vs NaCl
@@p<0.0005 vs NaCl
G.
GP
GL-TG
GL-DG
[14C-Gly]-Glycerolipids (pmol/10^6cell)
Iso
Iso + 4μ8C
NaCl
NaCl + 4μ8C
*p<0.001 vs Iso
Δp<0.001 vs Iso +4μ8C
*p<0.0001 vs Iso
Δp<0.05 vs Iso + 4μ8C
@p<0.01 vs NaCl
*p<0.0001 vs Iso
Δp<0.0001 vs Iso + 4μ8C
@p<0.0001 vs NaCl
H.
Iso
NaCl
Iso + 4μ8C
NaCl + 4μ8C
10μm
I.
Number of LD/cell
*p<0.0001 vs Iso
Δp<0.001 vs Iso+4μ8C
ΔΔp<0.0001 vs Iso+4μ8C
@p<0.05 vs NaCl
NaCl - - + +
4μ8C - 20 - 20 mM
J.
Area of LD (a.u.)
*p<0.05 vs Iso
**p<0.01 vs Iso
****p<0.0001 vs Iso
Δp<0.0001 vs Iso+4μ8C
@p<0.0001 vs NaCl
NaCl - - + +
4μ8C - 20 - 20 mM

Figure 3

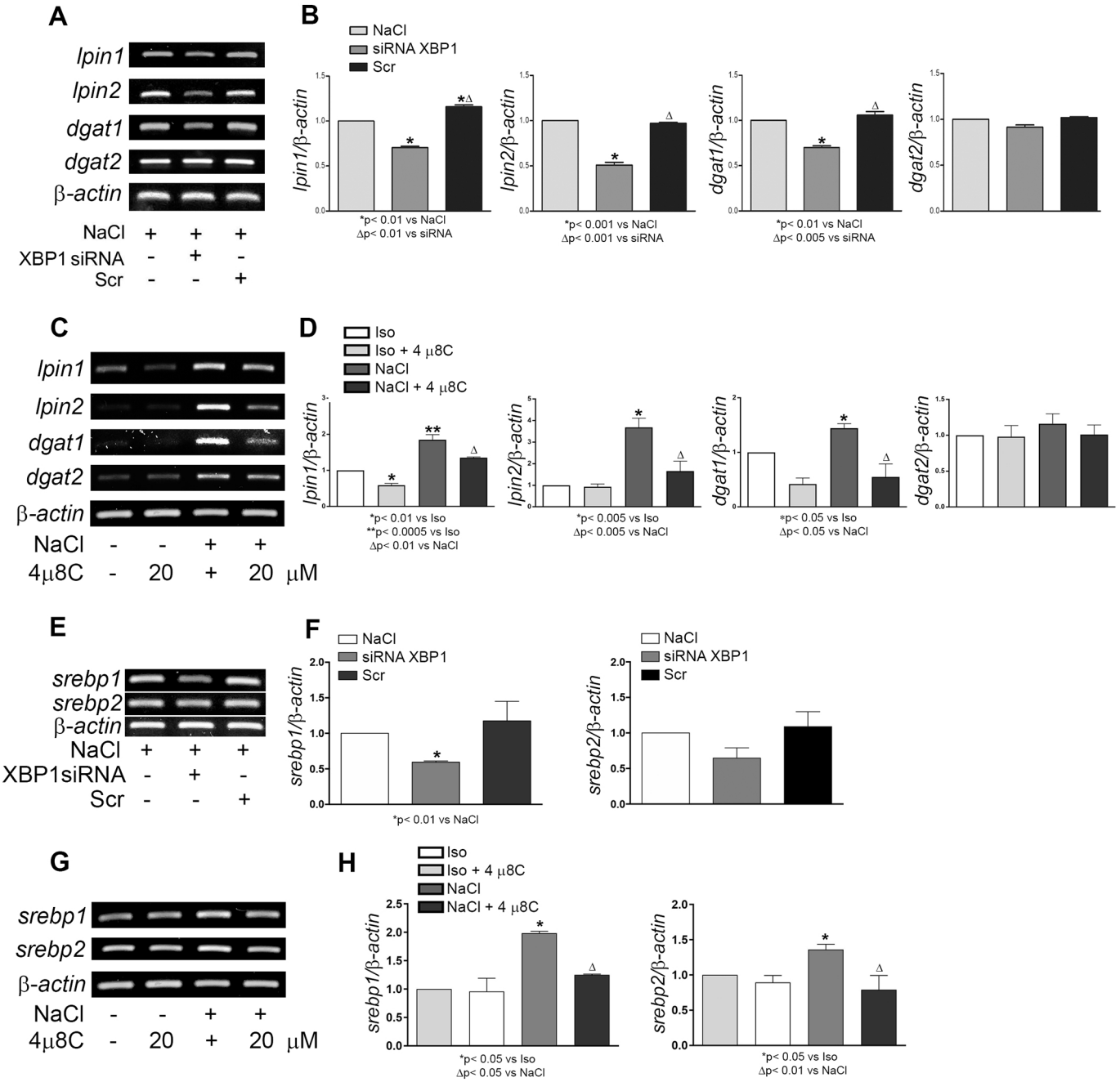
A
lpin1
lpin2
dgat1
dgat2
β-actin
NaCl + + +
XBP1 siRNA - + -
Scr - - +
B
NaCl
siRNA XBP1
Scr
lpin1/β-actin
lpin2/β-actin
dgat1/β-actin
dgat2/β-actin
*p< 0.01 vs NaCl
Δp< 0.01 vs siRNA
*p< 0.001 vs NaCl
Δp< 0.001 vs siRNA
*p< 0.01 vs NaCl
Δp< 0.005 vs siRNA
C
lpin1
lpin2
dgat1
dgat2
β-actin
NaCl - - + +
4μ8C - 20 + 20 μM
D
Iso
Iso + 4 μ8C
NaCl
NaCl + 4 μ8C
lpin1/β-actin
lpin2/β-actin
dgat1/β-actin
dgat2/β-actin
*p< 0.01 vs Iso
**p< 0.0005 vs Iso
Δp< 0.01 vs NaCl
*p< 0.005 vs Iso
Δp< 0.005 vs NaCl
*p< 0.05 vs Iso
Δp< 0.05 vs NaCl
E
srebp1
srebp2
β-actin
NaCl + + +
XBP1siRNA - + -
Scr - - +
F
NaCl
siRNA XBP1
Scr
srebp1/β-actin
srebp2/β-actin
*p< 0.01 vs NaCl
G
srebp1
srebp2
β-actin
NaCl - - + +
4μ8C - 20 + 20 μM
H
Iso
Iso + 4 μ8C
NaCl
NaCl + 4 μ8C
srebp1/β-actin
srebp2/β-actin
*p< 0.05 vs Iso
Δp< 0.05 vs NaCl
*p< 0.05 vs Iso
Δp< 0.01 vs NaCl

Figure 4

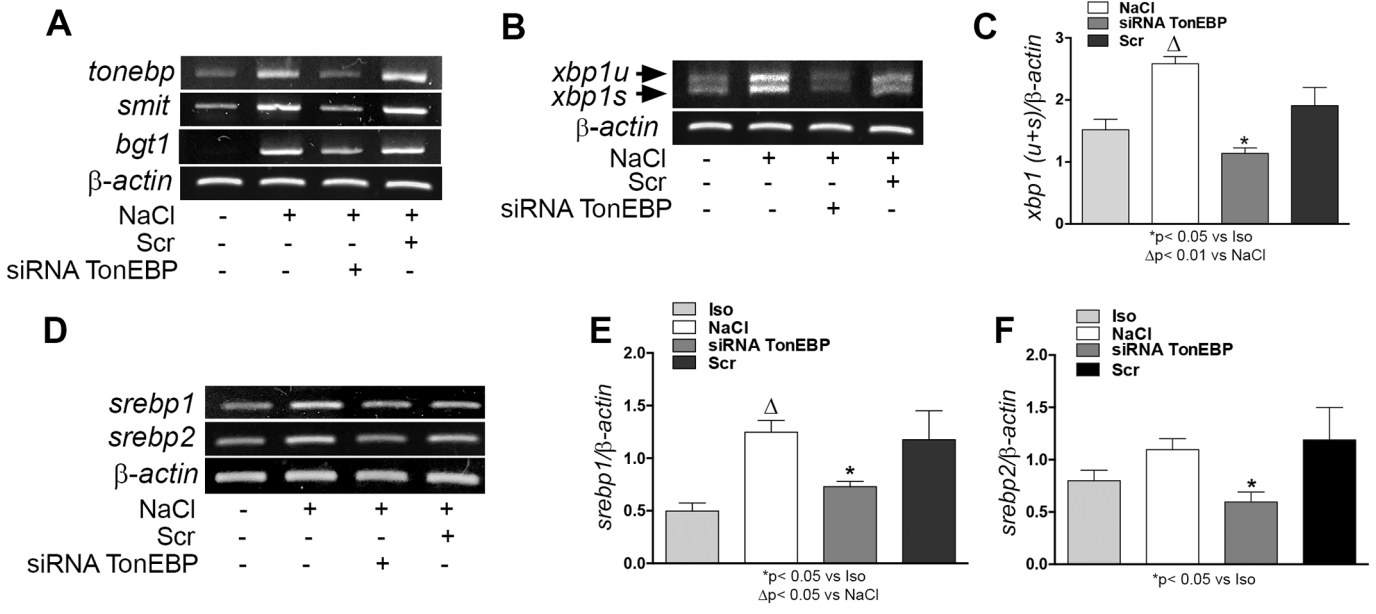
A
tonebp
smit
bgt1
β-actin
NaCl - + + +
Scr - - - +
siRNA TonEBP - - + -
B
xbp1u
xbp1s
β-actin
NaCl - + + +
Scr - - - +
siRNA TonEBP - - + -
C
Iso
NaCl
siRNA TonEBP
Scr
xbp1 (u+s)/β-actin
Δ
*
*p< 0.05 vs Iso
Δp< 0.01 vs NaCl
D
srebp1
srebp2
β-actin
NaCl - + + +
Scr - - - +
siRNA TonEBP - - + -
E
Iso
NaCl
siRNA TonEBP
Scr
srebp1/β-actin
Δ
*
*p< 0.05 vs Iso
Δp< 0.05 vs NaCl
F
Iso
NaCl
siRNA TonEBP
Scr
srebp2/β-actin
*
*p< 0.05 vs Iso

Figure 5

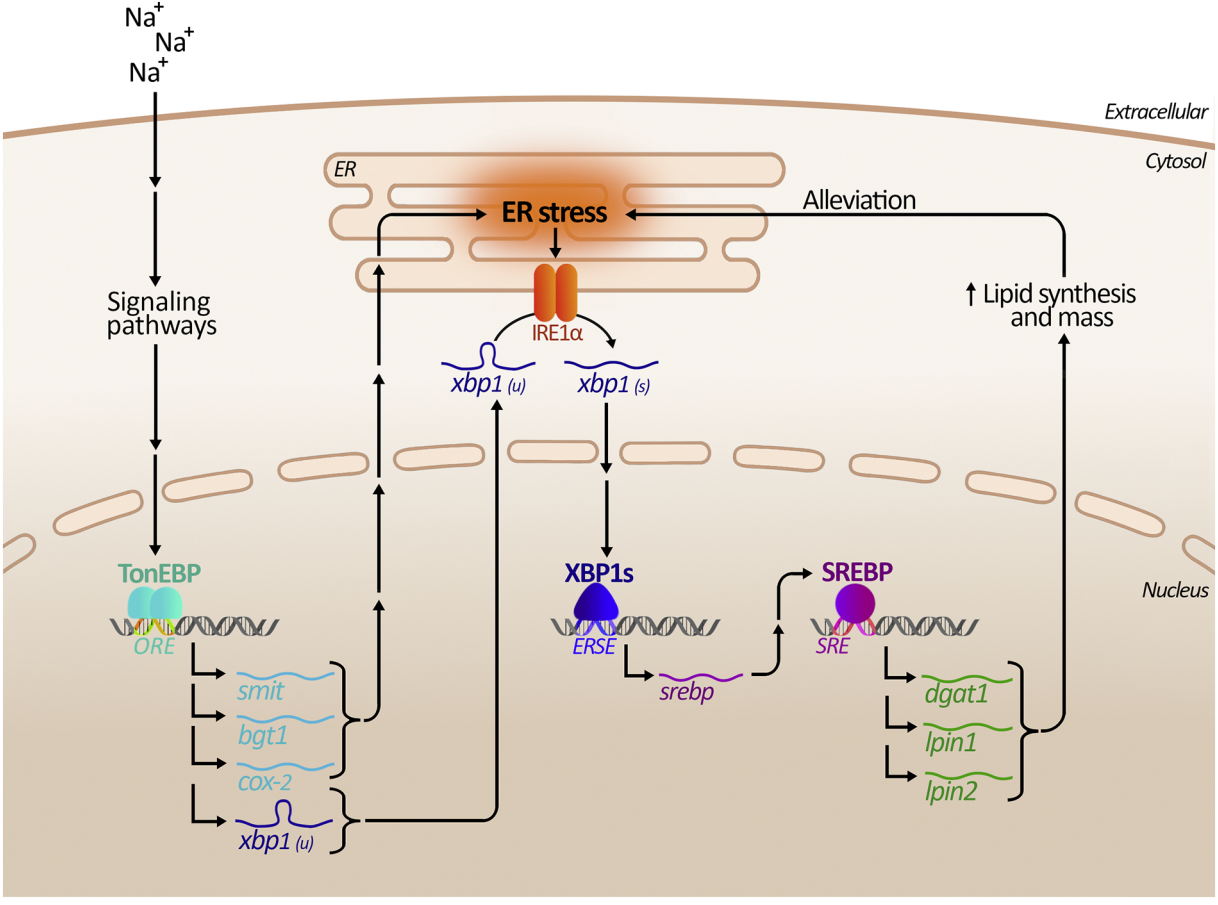
Na+
Na+
Na+
Extracellular
Cytosol
ER
ER stress
Alleviation
Signaling pathways
IRE1α
xbp1 (u)
xbp1 (s)
↑ Lipid synthesis and mass
TonEBP
ORE
XBP1s
ERSE
SREBP
SRE
Nucleus
smit
bgt1
cox-2
xbp1 (u)
srebp
dgat1
lpin1
lpin2

Figure 6